Experimental study of the mechanical properties of intact and tectonic coal via compression of a single particle

Jun Dong, Yuanping Cheng *, Biao Hu, Congmeng Hao, Qingyi Tu, Zhengdong Liu

Key Laboratory of Gas and Fire Control for Coal Mines (China University of Mining and Technology), Ministry of Education, Xuzhou 221116, China
National Engineering Research Center for Coal Gas Control, China University of Mining and Technology, Xuzhou, Jiangsu 221116, China
School of Safety Engineering, China University of Mining and Technology, Xuzhou, Jiangsu 221116, China

ARTICLE INFO

ABSTRACT

Mechanical properties of coal are key factors that influence coal mining and methane extraction. Considering the difficulties in obtaining the mechanical properties of the tectonic coal and some intact coal, uniaxial compression tests were conducted on both types of coal particles in the size range of 0.2–4.0 mm. The force-displacement curves, effective elastic moduli and tensile strengths of the intact and tectonic coal particles were obtained. The power functions were used to describe the distributions of the effective elastic moduli and tensile strengths with the diameters of both coal particles. Statistical distributions of the effective elastic modulus and tensile strength for each coal sample with different particle size intervals were also plotted using a logistic function. The test results revealed that the intact coal shows obvious brittleness, whereas the tectonic coal has a smaller brittleness. The obtained effective elastic modulus and tensile strength of the intact coal are 2.72–4.57 and 2.86–6.35 times those of the tectonic coal, respectively, with particle diameters of 0.2–4.0 mm. The characteristics of low strength and large deformation of the tectonic coal would result in greater difficulty of methane extraction and increased risk during coal mining. Some considerations on the structural model of the tectonic coal and measures to enhance the methane extraction efficiency and reduce the risk of mining were also analyzed.

© 2017 Elsevier B.V. All rights reserved.

1. Introduction

Coal and coalbed methane are valuable energy sources that are widely used for electricity generation, domestic fuel and steelmaking [1]. The strength and deformation characteristics of coal have significant influences on the production rate of coal, the support pattern of the roof, the evolution of the fractures and the extraction rate of methane [2]. Thus, it can be concluded that the mechanical properties of coal have a direct influence on the production capacity of coal, the safety of coal mining and the efficiency of methane extraction.

To study the mechanical properties of raw coal, large blocks of intact coal are usually collected and processed into cylindrical or cube samples. Next, a press machine can be used to perform uniaxial and three axial compression tests of the coal samples. The deformation sensor and force transducer are used to monitor the strain and stress of the coal samples. Some mechanical properties, including elastic modulus, Poisson's ratio and compressive strength, can be obtained from the stress-strain curve [3]. Most anthracite is easy to process into standard coal specimens because it has high strength, which inhibits its breakage in the machining process. However, large blocks of intact coal are not easy to obtain in many coal mines, and some bitumite is not hard enough to process into standard test specimens.

In the process of coal formation, a part of intact coal was subjected to tectonic stress, forming deformed coal with new structural characteristics; such coal is named tectonic coal [4]. The tectonic coal is usually distributed in layers and trapped between intact coal layers. Tectonic coal has the characteristics of low strength, high methane content and strong stress sensitivity. The area of tectonic coal is prone to coal and gas outburst accidents, and methane extraction in this area is of low efficiency [4]. Thus, study on the mechanical properties of tectonic coal is of tremendous practical value.

However, the tectonic coal cannot be drilled and processed into cylindrical samples because it is soft and easy to break. The tectonic coal can be pressed into cylindrical samples using a mold; however, the compressed sample cannot reflect the original state of the tectonic coal. Thus, it is difficult to obtain valid mechanical properties of the tectonic coal from traditional methods.

To solve the above problems, performing tests on coal particles is a good choice because the intact and tectonic coal grains are easy to obtain in all coal mines. Some scholars studied the mechanical properties of granules, including polystyrene, Al_2O_3, synthetic zeolite, sodium benzoate, iron ore and sodium chloride [5–9]. Research on coal particles, however, is not common; an exception is the report of Zhong et al. [10], who studied the effects of particle size on the strength parameters of

intact brown coal using a uniaxial testing device. In addition, few data have been reported for the mechanical properties of tectonic coal, and the relations of the mechanical parameters between the intact and tectonic coal have not drawn much attention.

Considering the difficulties in obtaining the mechanical properties of the tectonic coal and some intact coal using cylindrical or cube samples, this paper focused on determining the mechanical properties using rounded coal particles. A uniaxial testing device was used to conduct uniaxial compression on a single coal particle. The force-displacement curves of the intact and tectonic coal grains were analyzed, accompanied by pictures taken by a video microscope. The effective elastic moduli and tensile strengths of the intact and tectonic coal particles were calculated. The relationships among these mechanical parameters between the intact coal and tectonic coal were quantitatively analyzed. Based on the differences in the mechanical properties of both coal samples, some considerations on the structural model of tectonic coal, measures to reduce the risk of coal mining and enhance the efficiency of methane extraction were proposed.

2. Experimental details

2.1. Coal samples

The bitumite of the Qinan coal mine in the Chinese Huaibei Coalfield was collected as the experimental coal samples. Both intact coal and tectonic coal were collected from the same location of the 1016 working face. Fig. 1 shows the clumpy intact and tectonic coal samples. The intact coal is bright, with a clear bedding structure, and is uneasy to break, whereas the tectonic coal is dark, with unclear structure, and is easy to break into powders by hand. To study the composition and adsorption properties of the coal samples, proximate analysis were conducted and adsorption constants were obtained. The proximate analyses of the samples followed ISO recommendations (ISO Standard 11,722-1999 for moisture, ISO Standard 1171-1997 for ash, and ISO Standard 562-1998 for volatile matter and fixed carbon) and used a 5E-MAG6600 automatic proximate analyzer (Changsha Kaiyuan Instruments, China). High-pressure volumetric equipment was used to test the methane adsorption capacity of coal samples at 30 °C following the MT/T752–1997 method for determining the methane adsorption capacity in coal (China Department of Coal Industry, 1997). Langmuir isotherm at 30 °C was drawn, and the Langmuir parameters V_L and P_L can be obtained. The proximate analysis and the adsorption constants of the experimental samples are shown in Table 1. It can be seen that the ash content of the tectonic coal is apparently higher than that of the intact coal, which may be caused by the tectonic movement. The tectonism also changes the pore structure, porosity and skeleton of coal [4],

which may have a significant influence on the mechanical behavior of coal.

To conduct the uniaxial compression tests of coal particles, the intact coal specimen was smashed, and then, the particles were separated by sieving into different size fractions, including 0.2–1.0 mm, 1.0–2.0 mm and 2.0–4.0 mm. The tectonic coal was directly sieved to the same size fractions as the intact coal particles. To reduce the error caused by particle shape, an XDC-10 W-T1000 CCD video microscope manufactured by Suzhou Beitejia Photoelectric Technology Co., Ltd. (Fig. 2) was used to select approximately spherical particles for the uniaxial compression tests. The magnification of the video microscope is 10–133, and the resolution is 9.8 megapixels. The video microscope can also be used to measure millimeter-scale via image processing software.

2.2. Experimental setup and procedures

Mechanical properties of coal samples were tested using a TY8000-A uniaxial testing device manufactured by Jiangsu Tianyuan Test Equipment Co., Ltd. (Fig. 2). A single coal particle was placed between two rigid platens made of No. 45 steel (China national standard). The lower platen was immovable, and the upper platen was moved by a servo motor driving the screw. The applied force was measured by a BAB-5MT load transducer manufactured by Transcell, and the load resolution was up to 5×10^{-4} N. When the upper platen sensed the coal particle by a tiny force of 2×10^{-3} N, the testing system started to record the loading force and the displacement of the platen. The displacement was measured by a photoelectricity displacement coder with the stroke resolution of 1 μm produced by Panasonic. To ensure the quasi-static compression of coal particles, a loading rate of 0.15 mm/min was adopted to move the upper platen; this loading rate was far smaller than that used by some researchers [6,7,9–11]. When the loading force decreased to the half of the tested maximum of the particle, the testing system automatically stopped compressing the coal particle to avoid contact between the two platens and protect the pressure transducer of the testing device. The video microscope was also used to monitor the deformation of the coal particle during the experimental process.

This research focuses on the force-displacement relations, effective elastic moduli and tensile strengths of the intact and tectonic coal particles. The well-established theories for calculating the effective elastic modulus and tensile strength are the Hertz equation [5,12] and the Hiramatsu equation [13], respectively. A key parameter in the two equations is the radius of a particle, i.e., spheres are better for the uniaxial compression tests if these theories are desired to be adopted. Thus, we selected approximately spherical particles for the uniaxial compression test and treated them as spheres. When the upper platen contacted a coal particle, we used the video microscope to measure the distance
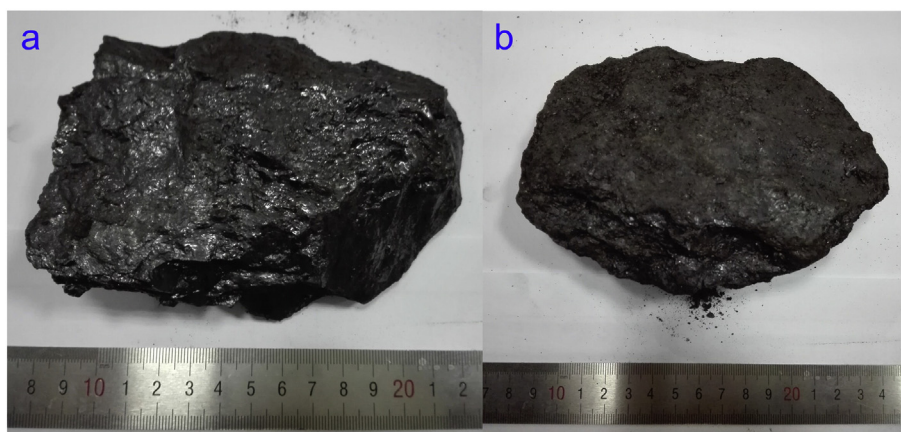

Fig. 1. Clumpy intact and tectonic coal samples from the Qinan coal mine: a) Intact coal; b) Tectonic coal.

Table 1
Proximate analysis and adsorption constants of intact and tectonic coal samples.

Coal sample	Proximate analysis (wt%)				Adsorption constants	
	Moisture	Ash	Volatile matter	Fixed carbon	V_L (m³/t)	P_L (MPa)
Intact coal	1.01	7.73	31.74	59.52	16.070	1.115
Tectonic coal	1.80	39.65	21.04	37.51	16.071	0.861

Footnote: Moisture, ash, volatile matter and fixed carbon are on air-dry basis; V_L is the Langmuir volume; P_L is the Langmuir pressure.

between the two platens, which was thought to equal to the diameter of the coal particle [10]. Although approximately spherical coal particles were selected for the experiment, the discreteness of the samples cannot be eliminated, and a sufficient number of coal particles should be used to reduce the error. Portnikov et al. [9] and Ribas [14] believed that 50 particles are sufficient to provide a satisfactory mechanical property for their experiments. In this study, 198 intact coal particles and 140 tectonic coal particles were measured using the compression tests. For the intact coal, 67, 86 and 45 particles with the size ranges of 0.2–1.0 mm, 1.0–2.0 mm and 2.0–4.0 mm, respectively, were measured, and the corresponding numbers were 41, 45 and 48 with the same size groups for the tectonic coal, respectively. The sample sizes were believed to be adequate to present the mechanical properties of the particles because more tests had little effect on the results.

3. Results and discussion

3.1. Force-displacement curve

Fig. 3 illustrates a typical force-displacement curve for an intact coal particle. At the former stage (Point O—Y), the force-displacement curve shows a nonlinear relation. After the initial nonlinear section, the force-displacement curve shows a linear relation until the peak point B. It is postulated that the particle undergoes elastic (Hertzian) deformation during the initial nonlinear region and plastic deformation during the linear relation of the force-displacement curve [5]. The yield point Y is the demarcation point of nonlinear and linear regions, which can be

determined by reversely deducing the linear force-displacement relation and obtaining the deviation point. There is no apparent change in the coal particle in the nonlinear stage, except for a growing contact area between the grain and the platens (see Fig. 3a and b). In the linear stage, cracks were generated and gradually expanded with the increasing energy accumulated in the coal particle (see Fig. 3c). At the peak point B, the coal grain with macro-cracks was no longer able to resist the force of the platen. In a short time, the coal particle burst into two or more pieces to release the accumulated energy (see Fig. 3d), and the force decreased rapidly, accompanied by a loud noise. Because of the rapid decline in loading force to a low level, the testing system stopped to protect the force transducer from damage. Overall, the intact coal has a large compressive capacity and small deformation, showing a high slope of the curve between point O and point B. It also ruptures quickly with a rapid release of energy at the peak point, showing obvious brittleness.

Compared with the intact coal, the force-displacement relation of the tectonic coal particle is more complex (see Fig. 4). First, a nonlinear relation followed by a linear section exhibits until the first peak point B. In this stage, the coal particle has unobvious change (see Fig. 4a and b), but minor cracks must be generated in the coal grain because of the subsequent decrease in the loading force of the testing system. At the first peak point B, the primary breakage occurred within the tectonic coal particle, and the coal particle was no longer able to resist a greater force. However, there was no apparent crack throughout the coal particle, and it did not break into several pieces rapidly with a loud noise as the intact coal sample. The force decrease after the first peak
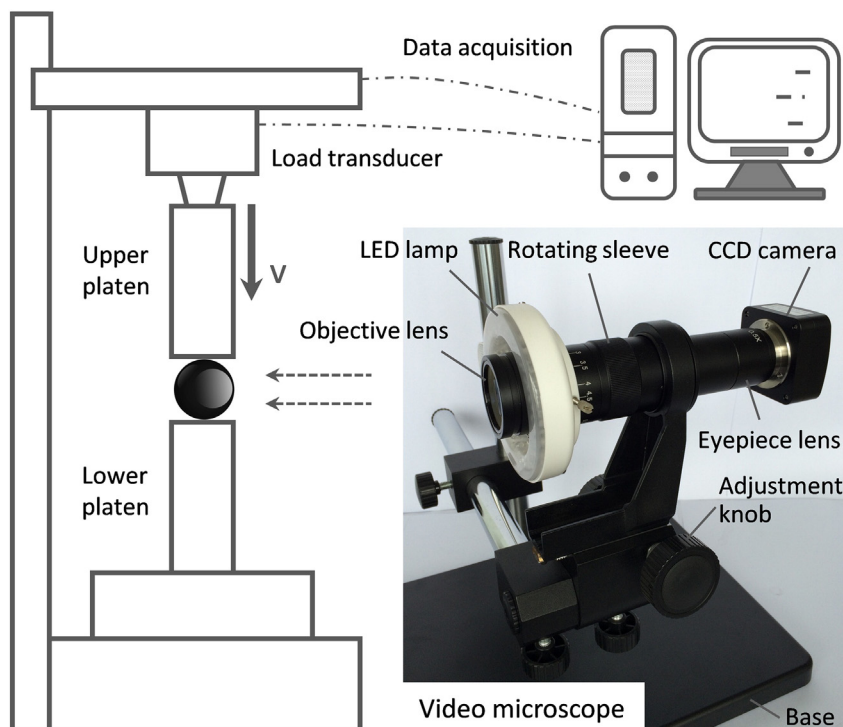

Fig. 2. Video microscope and schematic diagram of the experimental setup.
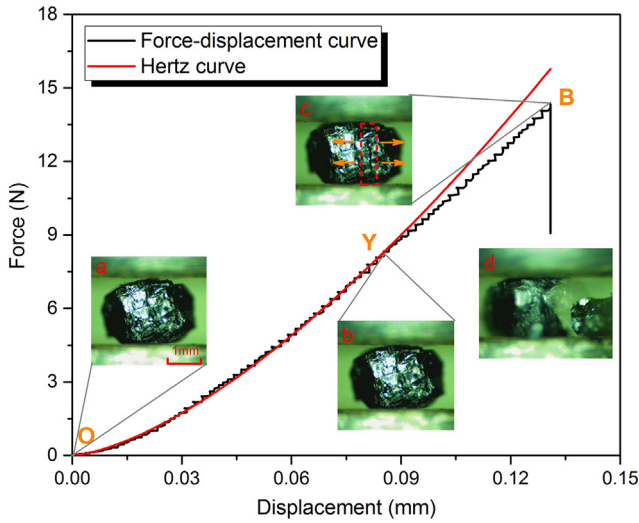
Fig. 3. Typical force-displacement curve for an intact coal particle.

point was much slower than that of the intact coal. It can be concluded that the energy accumulated in the tectonic coal particle released slowly. Because the force decrease value of the fractured coal sample was smaller than half of the tested maximum force, the testing system did not stop after point B. The coal sample was continuously broken and rearranged, and the contact area between the sample and the platens increased rapidly (see Fig. 4c). Thus, the loading force fluctuated with the increasing displacement, accompanied by continuous energy accumulation and release. At point C, the coal sample was almost compacted (see Fig. 4d), and the upper platen sensed the lower one, causing the loading force to increase sharply. To protect the load transducer, we manually stopped the test after the coal sample was compacted. The debris of the tectonic coal sample could not be recovered. The fractured coal particle had a large morphological change after the force was removed (see Fig. 4e) compared with its initial state. Overall, the tectonic coal has small compressive capacity and large deformation at the first peak point, showing a small slope of the curve between point O and point B. It ruptures slowly with a small release of energy at the first peak point, showing a smaller brittleness compared with that of the intact coal particle.

Both of the intact and tectonic coal particles undergo elastic deformation during the initial parabolic region of the force-displacement
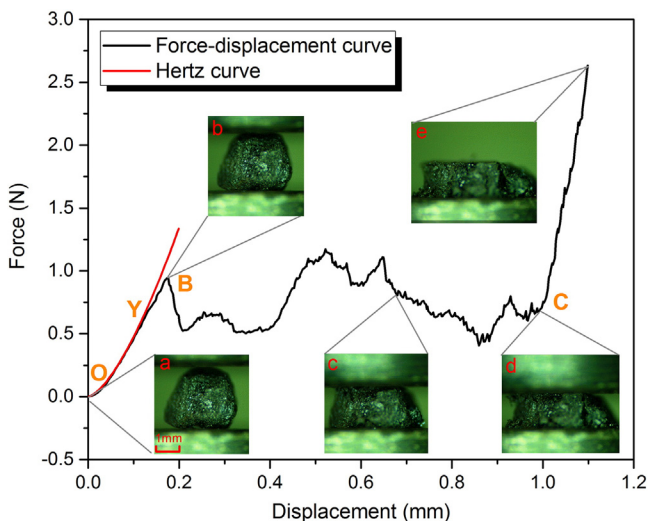
curve. If the loading force is disburdened, then the coal particle can recover to the initial state absolutely. As the displacement of coal particle increases, plastic deformation is initiated so that the measured force increases linearly with the increasing displacement [5]. The coal grain undergoes unrecoverable deformation when the force-displacement curve reaches the linear section.

3.2. Effective elastic modulus

Elastic modulus is a typical parameter for describing the elastic deformation characteristic of a material. For a cylindrical material, the elastic modulus is easy to obtain by calculating the slope of the stress-strain curve during elastic deformation. For the spherical material, however, the contact area between the grain and the platens is changing, and the stress cannot be easily obtained. Thus, the stress-strain curve and the elastic modulus cannot be directly obtained from the force-displacement curve of a spherical coal grain. Nevertheless, we can still obtain the elastic deformation characteristic of the coal particles.

For the contact of an elastic spherical particle and rigid platens, Hertz theory can be used to describe the force-displacement relationship, which is given by [5,12]

$$F_{el} = \frac{\sqrt{2}}{3} E^* R^{1/2} s^{3/2} \tag{1}$$

where F_{el} is the elastic contact normal force, N; R is the radius of coal particle, mm; s is the total platen displacement, mm; and E^* is the effective elastic modulus, MPa, which is related to the elastic modulus and the Poisson's ratio:

$$E^* = \frac{E}{1-\upsilon^2} \tag{2}$$

where E is the elastic modulus, MPa; and υ is the Poisson's ratio.

It can be seen that the effective elastic modulus has a certain relationship with the elastic modulus. If the Poisson's ratio of a material is known, then the effective elastic modulus can be transferred to the elastic modulus. The Poisson's ratio of the intact coal is relatively easy to obtain by testing the stress-strain relation of a cylindrical raw coal sample. The Poisson's ratio of the tectonic coal, however, is difficult to obtain because a cylindrical raw coal sample cannot be acquired. Thus, we compare the effective elastic moduli of the intact coal and tectonic coal in the following part.

With the measured elastic contact force and platen displacement at the yield point as well as the particle radius, the effective elastic modulus of the coal particle can be calculated using Eq. (1). The Hertz curves for the intact and tectonic coal particles are also illustrated in Fig. 3 and Fig. 4, respectively.

Fig. 5 compares the effective elastic moduli of the intact and tectonic coal particles, and the values of both coal samples increase with the decreasing particle size. The effective elastic moduli of most intact coal particles are higher than those of the tectonic coal with the same particle size, i.e., the tectonic coal is easier to deform under the same loading force. The size effect can be explained by the influence of amounts of macropores and minor cracks [10]. For smaller coal particles, the probability of the occurrence of macropores and minor cracks is lower because some of them may be eliminated by the grinding and sieving of the coal samples.

By assuming a constant effective elastic modulus for very large particles and a final value when the particle size goes to zero, Portnikov and Klaman [11] proposed an exponential function to fit the change in the effective elastic moduli with particle diameter. If a smaller coal particle is thought to have a higher effective elastic modulus, then the power function can also be used to describe the relationships between the effective elastic modulus and the particle size. By comparison, we found that the power function has a higher correlation coefficient for coal particles in the size range of 0.2–4.0 mm. Thus, the power function
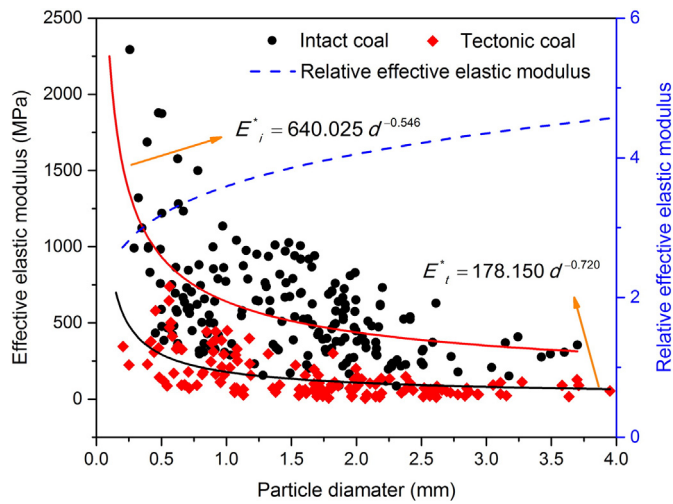

Fig. 4. Typical force-displacement curve for a tectonic coal particle.

Fig. 5. Measured and regressed values of effective elastic moduli for intact and tectonic coal particles as a function of particle diameter.

Fig. 6. Cumulative distribution of the effective elastic moduli for intact and tectonic coal particles.

was chosen to fit the effective elastic moduli for both intact and tectonic coal particles because of its better goodness of fit:

$$E^* = k_{E^*} \cdot d^{n_{E^*}} \tag{3}$$

where d is the diameter of a coal particle, mm; k_{E^*} and n_{E^*} are constants, which depend on the properties of coal samples. The fitting parameters of both intact and tectonic coal particles are given in Table 2.

To obtain a quantitative deformation relationship between the intact coal and the tectonic coal, we define the relative effective elastic modulus as the ratio of the effective elastic modulus of the intact coal to that of the tectonic coal, which can be calculated using the fitting parameters in Table 2 and is also illustrated in Fig. 5. It can be seen that the relative effective elastic modulus increases with the increasing coal particle size, with the value changing from 2.72 to 4.57 for coal particle diameter in the range of 0.2–4.0 mm. For particles with a diameter of 1 mm, the relative effective elastic modulus is 3.59, i.e., the strain of the tectonic coal is 3.59 times that of the intact coal under the same external force, if the difference in Poisson's ratios is neglected.

The above analysis focused on the relationship between the effective elastic modulus and the particle size. For a coal particle, it is important to determine the distribution probability of effective elastic modulus. Thus, the statistical distribution of the effective elastic modulus for each coal sample should be determined. For the experiments of different particle size intervals, the cumulative distributions for the effective elastic moduli of both coal samples are plotted in Fig. 6. The cumulative probability was plotted by the ratio of numbers of particles that have smaller effective elastic moduli at any effective elastic modulus to the total measured numbers of particles for each size fraction. The experimental data for each distribution were plotted for only ten narrow effective elastic moduli to clarify the variation tendency. Next,
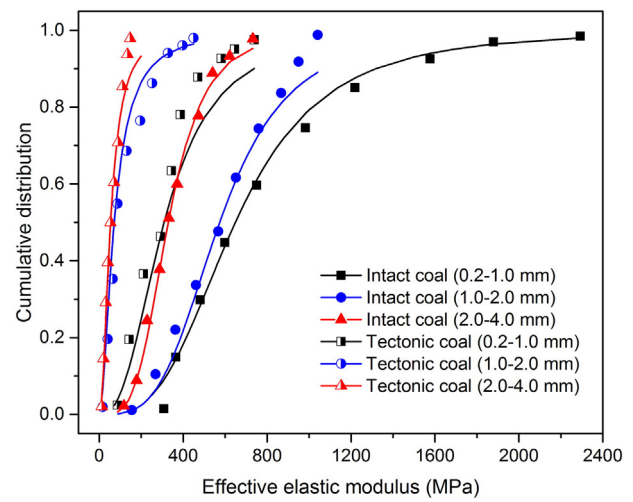
we defined the distributions mathematically in a similar manner as that described by Portnikov and Kalman [11] using the following logistic function:

$$S_{E^*} = 1 - \frac{1}{1 + (E^*/E^*_{50})^{D_{E^*}}} \tag{4}$$

where S_{E^*} is the probability of the particle with a smaller effective elastic modulus; E^*_{50} is the median effective elastic modulus of the distribution, MPa; and D_{E^*} is the distribution wideness (as D_{E^*} becomes larger, the distribution becomes narrower).

By fitting Eq. (4) to each set of experimental data in Fig. 6, the logistic function parameters were obtained, as summarized in Table 3. The fitting curves are also illustrated with solid lines in Fig. 6. It can be seen that the curves are shifted to the left with increasing particle sizes for both coal samples, i.e., a larger coal particle has a smaller effective elastic modulus, which is in accordance with the size effect analyzed above. In addition, the curve of tectonic coal for each size friction is on the left of that of the intact coal, showing a higher effective elastic modulus for the intact coal. The parameter D_{E^*} shows random distribution, which is in agreement with the research results of Portnikov and Kalman [11]. The parameter E^*_{50}, undoubtedly, shows a decreasing trend with the increasing coal particle size.

3.3. Tensile strength

The strength of a material is an important parameter for describing its mechanical property. When the loading force reaches the first peak point, the intact coal particle shows an obvious fracture across the top and bottom, while the tectonic coal sample does not have obvious change. Regardless of the state at the peak point, the structures of

Table 2
Fitting parameters of Eqs. (3) and (6) for intact and tectonic coal samples.

Coal sample	Property	Eq. (3)		Eq. (6)		R
		k_{E^*}	n_{E^*}	k_{σ_T}	n_{σ_T}	
Intact coal	E^*_i	640.025	−0.546			0.57
	$\sigma_{T,i}$			5.114	−0.905	0.76
Tectonic coal	E^*_t	178.150	−0.720			0.62
	$\sigma_{T,t}$			1.165	−1.171	0.75

Footnote: R denotes the goodness of fit. E^*_i and E^*_t denotes the effective elastic modulus for intact coal and tectonic coal, respectively. $\sigma_{T,i}$ and $\sigma_{T,t}$ denotes the tensile strength for intact coal and tectonic coal, respectively.

Table 3
Logistic function parameters of Eqs. (4) and (7) for intact and tectonic coal samples.

Coal sample	Particle size interval (mm)	Eq. (4)			Eq. (7)		
		E^*_{50} (MPa)	D_{E^*}	R	$\sigma^*_{T,\ 50}$ (MPa)	D_{σ_T}	R
Intact coal	0.2–1.0 mm	6.49	2.58	0.997	648.67	3.10	0.997
	1.0–2.0 mm	3.19	3.44	0.998	574.14	3.52	0.991
	2.0–4.0 mm	2.04	2.68	0.994	328.84	3.77	0.997
Tectonic coal	0.2–1.0 mm	1.53	2.01	0.975	309.12	2.53	0.953
	1.0–2.0 mm	0.34	1.72	0.993	71.42	1.80	0.976
	2.0–4.0 mm	0.15	2.63	0.995	53.98	2.01	0.993

both intact and tectonic coal samples are damaged, and they are no longer able to resist a greater force before being compacted.

Tensile strength is a representative parameter for evaluating the strength of a particle [13]. Based on experimental and analytical results obtained from tests on several types of rocks, Hiramatsu and Oka [13] suggested that the tensile strength of a particle can be defined as

$$\sigma_T = \frac{0.7 F_B}{\pi R^2} \quad (5)$$

where σ_T is the tensile strength of a particle, MPa; F_B is the contact normal force at the break point, N.

The tensile strengths of the intact and tectonic coal particles are illustrated in Fig. 7. The values of the intact coal are obviously higher than those of the tectonic coal, i.e., the tectonic coal is easier to rupture under the same loading force. The tensile strengths of the coal particles also exhibit a size effect, showing an increasing trend with decreasing particle size. The power function can also fit the obtained tensile strengths for intact and tectonic coal particles:

$$\sigma_T = k_{\sigma_T} \cdot d^{n_{\sigma_T}} \quad (6)$$

where k_{σ_T} and n_{σ_T} are also constants related to the properties of coal samples. The fitting parameters of the tensile strengths for both intact and tectonic coal particles are also given in Table 2. Similar to the relative effective elastic modulus, we define the relative tensile strength as the ratio of the tensile strength of the intact coal to that of the tectonic coal, which can also be calculated using the fitting parameters in Table 2, as illustrated in Fig. 7. It can be seen that the relative tensile strength also increases with increasing coal particle size, showing the value n_{σ_T} of the intact coal is higher than that of the tectonic coal. The relative tensile strength changes from 2.86 to 6.35 with increasing coal particle
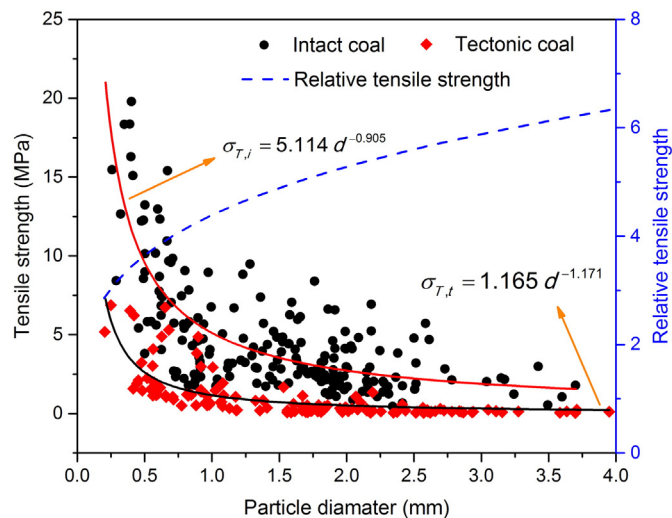
size in the range of 0.2–4.0 mm. For particles with a diameter of 1 mm, the relative tensile strength is 4.39, i.e., the force for rupturing the tectonic coal is only 22.8% of that for the intact coal.

For the experiments of different particle size intervals, the cumulative distributions for the tensile strength of both coal samples are presented in Fig. 8. The experimental data for each distribution were also plotted for ten narrow tensile strengths to clarify the results. Next, the following logistic function was used to fit the distribution of tensile strength:

$$S_{\sigma_T} = 1 - \frac{1}{1 + (\sigma_T / \sigma_{T,\ 50})^{D_{\sigma_T}}} \quad (7)$$

where S_{σ_T} is the probability of the particle to break; $\sigma_{T,\ 50}$ is the median tensile strength of the distribution, MPa; and D_{σ_T} is the distribution wideness.

By fitting Eq. (7) to each set of experimental data in Fig. 8, the logistic function parameters were obtained, as summarized in Table 3. The solid fitting curves for larger coal particles are also closer to the left coordinate axis, and the curve of the intact coal with a particle size of 2.0–4.0 mm is located to the right of that of the tectonic coal with a particle size of 0.2–1.0 mm. The parameter D_{σ_T} shows a random distribution and can be assumed to be independent of particle size [11]. The parameter $\sigma_{T,\ 50}$ increases with the decreasing coal particle size, further confirming the size effect.

3.4. Some considerations on tectonic coal

For the estimation of methane extraction and safety evaluation of coal mining, it is necessary to understand the structural model of coal and the process of methane migration. Previous studies were focused on the intact coal, the structure of which can be simplified into regular models, including the cube model and the matchstick model [15]. In other words, the intact coal is simplified as a dual-porosity system consisting of coal matrix and surrounding fractures [16]. The fracture system is the occurrence site and the flow channel for free methane, and the methane migration follows Darcy's law. The methane flow through the coal matrix is believed to be concentration-driven and follows Fick's law [17–19]. Methane in the coal matrix experiences the processes of diffusion and seepage before flowing into boreholes or well drillings.

Coal matrix blocks are not separated from each other but are connected by solid rock bridges [20]. Because of the large elastic modulus and strength, the solid rock bridges have high ability to resist deformation, enabling the fractures to maintain a flat shape and a
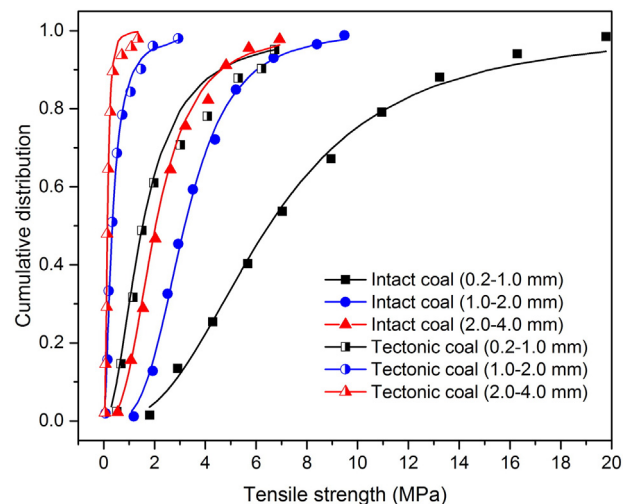
Fig. 7. Measured and regressed values of tensile strengths for intact and tectonic coal particles as a function of particle diameter.

Fig. 8. Cumulative distribution of the tensile strengths for intact and tectonic coal particles.

certain aperture, even at much higher stress [21]. Thus, methane seepage in the fractures plays an important role in the process of methane migration. Based on the cube or matchstick models, many scholars proposed a variety of coal permeability models in the last few decades to describe the process of methane seepage [22–30]. These permeability evolution models have been widely used for the estimation of methane extraction and safety evaluation of coal mining.

However, no suitable structural model or permeability model has been proposed for tectonic coal. From the obtained effective elastic modulus and tensile strength of tectonic coal, the values are far less than those of the intact coal. It is easy to imagine that an obvious matrix block and fracture system cannot easily form in tectonic coal under the same reservoir environment as intact coal. Because of the small strength and effective elastic modulus, the fractures of tectonic coal are subject to strong compressive deformation and cannot form a flat shape, especially when the depth of the coal seam is deeper with larger crustal stress. The fractures may become columnar or even be eliminated.

If the fractures of tectonic coal still exist, then the tectonic coal can also be simplified as a dual-porosity system; however, the fractures do not surround the matrix. The fractures are dispersed and relatively small. Thus, the permeability of tectonic coal is smaller than that of the intact coal. Alternatively, the contact area between the matrix and the fractures is very small, making the mass transfer between them difficult. Low permeability and difficulty in methane diffusion through coal matrix make it difficult to extract the methane from tectonic coal reservoir.

When the stress is very high, the fractures of tectonic coal may be eliminated. The tectonic coal forms single porous medium, and the whole tectonic coal reservoir becomes a large matrix. Under this circumstance, methane migration in the tectonic coal is diffusion driven by the concentration gradient, rather than methane seepage. If the diffusion coefficient of the tectonic coal is known, then it can be transformed into a diffusive permeability [31]. Next, Darcy's law can be used to evaluate the methane migration characteristics and extraction efficiency. The diffusive permeability can be calculated according to the following equation:

$$k = \frac{D\mu}{p} \qquad (8)$$

where k is the diffusive permeability, m^2; D is the diffusion coefficient, m^2/s; μ is the dynamic viscosity of methane, Pa·s; and p is the methane pressure, Pa. The diffusion coefficient of methane in coal is of the order of magnitude of 10^{-13}–10^{-9} m^2/s [32]. If the dynamic viscosity and the pressure of methane are 1.1×10^{-5} Pa·s and 10^6 Pa, respectively, then the diffusive permeability is of the order of magnitude of 10^{-24}–10^{-20} m^2/s, which is extremely low for methane migration or extraction.

So far, we cannot determine the structural model of the tectonic coal; however, the low strength and large deformation characteristics definitely make the extraction of methane from tectonic coal very difficult, which may result in high methane pressure gradient and increase the risk of coal mining significantly. Thus, measures should be taken to reduce or eliminate the danger of tectonic coal reservoir.

According to the Mohr-Coulomb law, loading or unloading can cause damage to coal, which leads to the formation and expansion of fractures and the increase in the contact area between the matrix and fractures. In this case, the tectonic coal is no longer single porous medium. The permeability of the tectonic coal increases dramatically, and the mass transfer between the matrix and the fractures becomes easy. Thus, methane in a coal reservoir can be extracted easily. Loading is difficult to perform in coal mines, and unloading is a more practical measure. Protective layer mining, hydraulic cutting, and construction of intensive extraction boreholes are effective measures to unload the crustal stress and enhance the permeability of tectonic coal. Relatively speaking, protective layer mining is more efficient because it has a wider stress relief range and a better effect [33]. If exploiting a layer of coal is not realistic, then mining of soft rock can also be considered, which has been achieved in the Chinese Luling coal mine. Overall, more attention should be paid to methane extraction and mining safety in coal mines with tectonic coal.

4. Conclusions

In this study, intact and tectonic coal particles with diameters in the range of 0.2–4.0 mm were used to conduct uniaxial compression tests using a uniaxial testing device. The force-displacement curves, effective elastic moduli and tensile strengths of the intact and tectonic coal particles were compared. The key findings of this study are summarized as follows:

(1) The intact coal particle ruptures quickly into several pieces with a rapid release of energy at the peak point, showing obvious brittleness. The tectonic coal particle ruptures slowly with a small release of energy at the first peak point, showing a smaller brittleness compared with the intact coal particle.

(2) The relations between the effective elastic moduli, tensile strengths and the diameters of both coal particles were fitted by power functions. The effective elastic modulus and tensile strength of the intact coal are 2.72–4.57 and 2.86–6.35 times those of the tectonic coal, respectively, with particle diameters of 0.2–4.0 mm, which means that the tectonic coal is easier to deform and rupture under the same force condition as the intact coal.

(3) The characteristics of low strength and large deformation of the tectonic coal have influences on the structural model and cause difficulty in methane extraction and higher risks during coal mining. Measures should be taken to enhance the methane extraction efficiency and reduce the mining risk of a tectonic coal reservoir.

Notes

The authors declare that we do not have any commercial or associative interest that represents a conflict of interest in connection with the work submitted.

References

[1] J. Dong, Y. Cheng, K. Jin, H. Zhang, Q. Liu, J. Jiang, B. Hu, Effects of diffusion and suction negative pressure on coalbed methane extraction and a new measure to increase the methane utilization rate, Fuel 197 (2017) 70–81.

[2] H.E. Lawson, D. Tesarik, M.K. Larson, H. Abraham, Effects of overburden characteristics on dynamic failure in underground coal mining, Int. J. Min. Sci. Technol. 27 (2017) 121–129.

[3] Y. Ju, Q. Zhang, J. Zheng, J. Wang, C. Chang, F. Gao, Experimental study on CH$_4$ permeability and its dependence on interior fracture networks of fractured coal under different excavation stress paths, Fuel 202 (2017) 483–493.

[4] S. Lu, Y. Cheng, W. Li, L. Wang, Pore structure and its impact on CH$_4$ adsorption capability and diffusion characteristics of normal and deformed coals from Qinshui Basin, International Journal of Oil, Gas and Coal Technology 10 (2015) 94–114.

[5] Y. Cheong, M. Adams, A. Routh, M. Hounslow, A. Salman, The production of binderless granules and their mechanical characteristics, Chem. Eng. Sci. 60 (2005) 4045–4053.

[6] S. Antonyuk, J. Tomas, S. Heinrich, L. Mörl, Breakage behaviour of spherical granulates by compression, Chem. Eng. Sci. 60 (2005) 4031–4044.

[7] R. Pitchumani, O. Zhupanska, G.M. Meesters, B. Scarlett, Measurement and characterization of particle strength using a new robotic compression tester, Powder Technol. 143 (2004) 56–64.

[8] W. Yu, T. Sun, Z. Liu, J. Kou, C. Xu, Effects of particle sizes of iron ore and coal on the strength and reduction of high phosphorus oolitic hematite-coal composite briquettes, ISIJ Int. 54 (2014) 56–62.

[9] D. Portnikov, H. Kalman, S. Aman, J. Tomas, Investigating the testing procedure limits for measuring particle strength distribution, Powder Technol. 237 (2013) 489–496.

[10] S. Zhong, F. Baitalow, P. Nikrityuk, H. Gutte, B. Meyer, The effect of particle size on the strength parameters of German brown coal and its chars, Fuel 125 (2014) 200–205.

[11] D. Portnikov, H. Kalman, Determination of elastic properties of particles using single particle compression test, Powder Technol. 268 (2014) 244–252.

[12] K.L. Johnson, Contact Mechanics, Cambridge university press, Cambridge, 1987.

[13] Y. Hiramatsu, Determination of the tensile strength of rock by a compression test of an irregular test piece, Int. J. Rock Mech. Min. Sci. 3 (1966) 89–99.

[14] L. Ribas, G.C. Cordeiro, R.D. Toledo Filho, L.M. Tavares, Measuring the strength of irregularly-shaped fine particles in a microcompression tester, Miner. Eng. 65 (2014) 149–155.

[15] S. Lu, Y. Cheng, W. Li, Model development and analysis of the evolution of coal permeability under different boundary conditions, J. Nat. Gas Sci. Eng. 31 (2016) 129–138.

[16] J.E. Warren, P.J. Root, The behavior of naturally fractured reservoirs, Soc. Pet. Eng. J. 3 (1963) 245–255.

[17] S. Harpalani, S. Ouyang, A new laboratory technique to estimate gas diffusion characteristics of naturally fractured reservoirs, 2nd North American Rock Mechanics Symposium, American Rock Mechanics Association, 1996.

[18] S. Zhou, Mechanism of gas flow in coal seams, J. China Coal Soc. (1990) 15–24.

[19] Z. Liu, Y. Cheng, J. Jiang, W. Li, K. Jin, Interactions between coal seam gas drainage boreholes and the impact of such on borehole patterns, J. Nat. Gas Sci. Eng. 38 (2017) 597–607.

[20] J. Liu, Z. Chen, D. Elsworth, X. Miao, X. Mao, Evaluation of stress-controlled coal swelling processes, Int. J. Coal Geol. 83 (2010) 446–455.

[21] H. Liu, J. Rutqvist, J.G. Berryman, On the relationship between stress and elastic strain for porous and fractured rock, Int. J. Rock Mech. Min. Sci. 46 (2009) 289–296.

[22] I. Gray, Reservoir engineering in coal seams: part 1-the physical process of gas storage and movement in coal seams, SPE Reserv. Eng. 2 (1987) 28–34.

[23] I. Palmer, J. Mansoori, How permeability depends on stress and pore pressure in coalbeds: a new model, SPE Annual Technical Conference and Exhibition, Society of Petroleum Engineers, 1996.

[24] J. Shi, S. Durucan, Drawdown induced changes in permeability of coalbeds: a new interpretation of the reservoir response to primary recovery, Transp. Porous Media 56 (2004) 1–16.

[25] X. Cui, R.M. Bustin, Volumetric strain associated with methane desorption and its impact on coalbed gas production from deep coal seams, AAPG Bull. 89 (2005) 1181–1202.

[26] H. Kumar, D. Elsworth, J. Liu, D. Pone, J.P. Mathews, Optimizing enhanced coalbed methane recovery for unhindered production and CO$_2$ injectivity, Int. J. Greenhouse Gas Control 11 (2012) 86–97.

[27] E. Robertson, R. Christiansen, A Permeability Model for Coal and Other Fractured, Sorptive-elastic Media, Idaho National Laboratory, 2006 INL/EXT-06-11830.

[28] L. Connell, Coupled flow and geomechanical processes during gas production from coal seams, Int. J. Coal Geol. 79 (2009) 18–28.

[29] L. Connell, M. Lu, Z. Pan, An analytical coal permeability model for tri-axial strain and stress conditions, Int. J. Coal Geol. 84 (2010) 103–114.

[30] S. Wang, D. Elsworth, J. Liu, Permeability evolution in fractured coal: the roles of fracture geometry and water-content, Int. J. Coal Geol. 87 (2011) 13–25.

[31] Y. Wang, S. Liu, Estimation of pressure-dependent diffusive permeability of coal using methane diffusion coefficient: laboratory measurements and modeling, Energy Fuel 30 (2016) 8968–8976.

[32] A. Gilman, R. Beckie, Flow of coal-bed methane to a gallery, Transp. Porous Media 41 (2000) 1–16.

[33] L. Wang, S. Liu, Y. Cheng, G. Yin, D. Zhang, P. Guo, Reservoir reconstruction technologies for coalbed methane recovery in deep and multiple seams, Int. J. Min. Sci. Technol. 27 (2017) 277–284.